Electronic Supplementary Material (ESI) for Physical Chemistry Chemical Physics.
This journal is © the Owner Societies 2015

Supporting Information for

Insight into the formation mechanism of graphene quantum dots and size effect on their capacitance behaviors

Yonghuan Liu,[a,b] Rutao Wang,[a] Junwei Lang[a] and Xingbin Yan[a*]

[a] *Laboratory of Clean Energy Chemistry and Materials, State Key Laboratory of Solid Lubrication, Lanzhou Institute of Chemical Physics, Chinese Academy of Sciences, Lanzhou 730000, P. R. China*

[b] *Graduate University of Chinese Academy of Sciences, Beijing 100080, P. R. China*

* Corresponding author. Tel.: +86 931 4968055; fax: +86 931 4968055.

E-mail address: xbyan@licp.cas.cn (X. B. Yan).

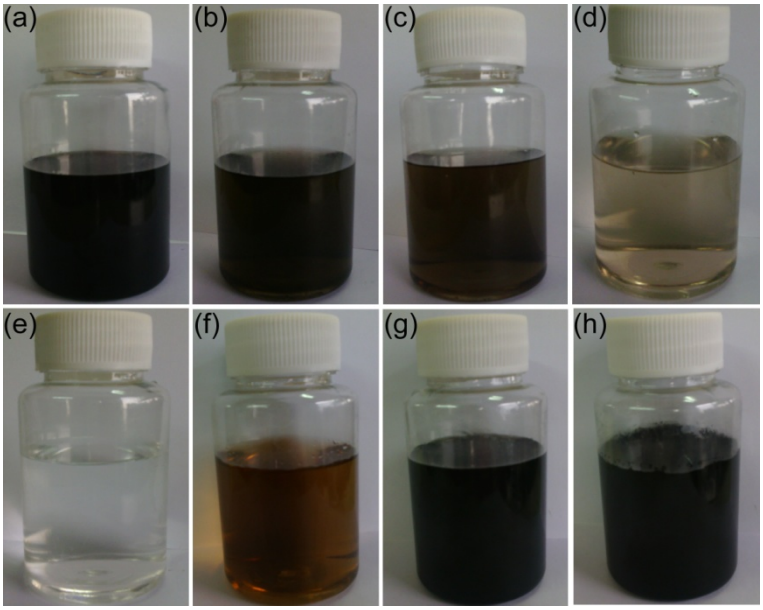

Fig. S1 The photographs of the varying degree chemical etching of GO sheets by adding only H_2O_2 at 180 °C for different reaction time: (a) 45 min, (b) 60 min, (c) 75 min, (d) 90 min, and (e) 120 min. (f) The photograph of the sample obtained by adding NaOH to replace of ammonia. The photographs of the samples obtained using N-RGO (g), and RGO-T (h) as raw materials to replace of GO, respectively.

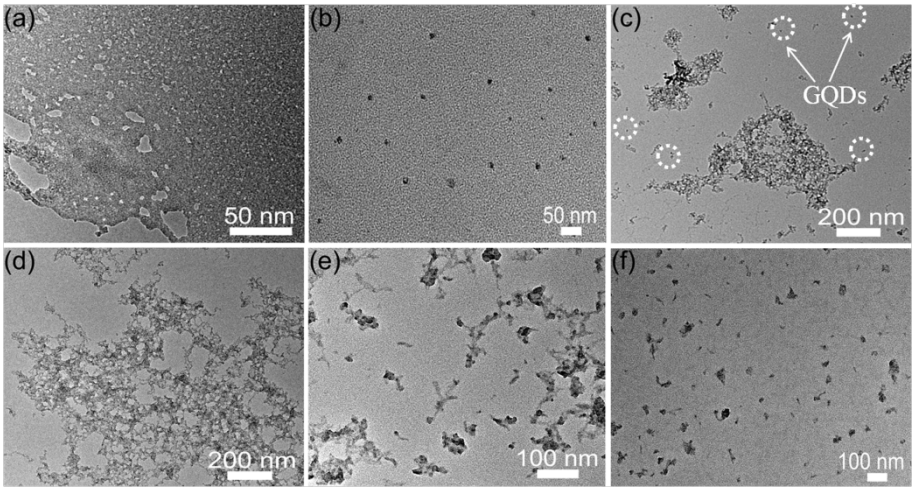

Fig. S2 TEM images of the samples: (a) filter cake obtained by removal of GQDs-1, (b) GQDs obtained by adding NaOH to replace of ammonia at similar pH value, (c) PRGO-2. TEM images of the samples obtained by etching GO sheets by adding H_2O_2 only at 180 °C for (d) 45 min, (e) 90 min, and (f) 105 min.

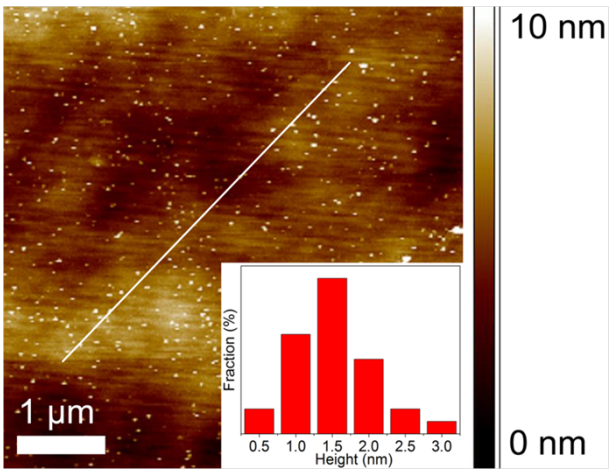

Fig. S3 AFM image of the smallest size sample of GQDs-1. Inset shows the corresponding height distribution.

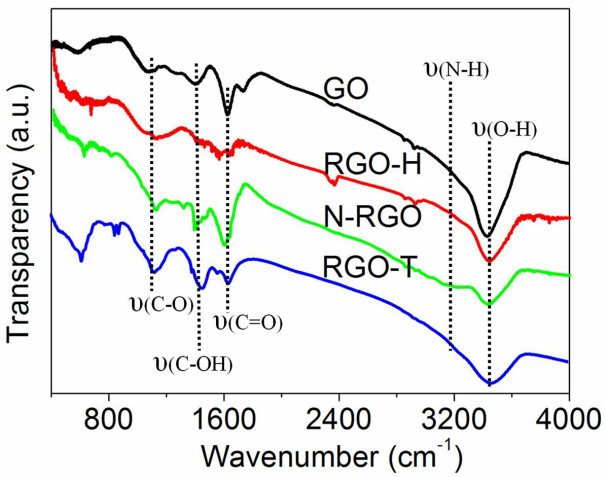

Fig. S4 FTIR spectra of pristine GO, RGO-H obtained by hydrothermal reduction at 180 °C for 8 h, N-RGO obtained by using hydrazine reduction at 95 °C for 1 h, and RGO-T prepared through thermal treatment under an argon atmosphere at 300 °C for 2 h.

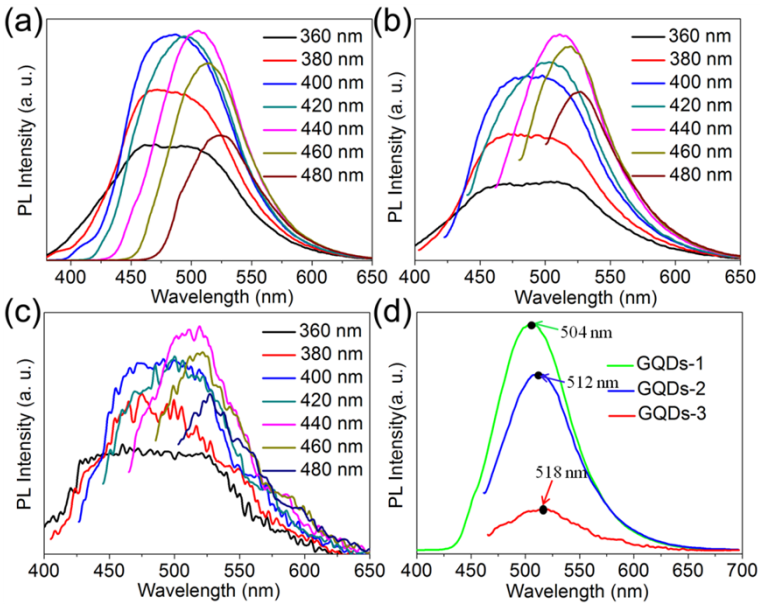

Fig. S5 PL spectra of GQDs series with different sizes at different excitation wavelengths from 360 nm to 480 nm: (a) PL spectra of GQDs-1, (b) PL spectra of GQDs-2, and (c) PL spectra of GQDs-3. (d) PL spectra of GQDs series at an excitation wavelength of 440 nm.

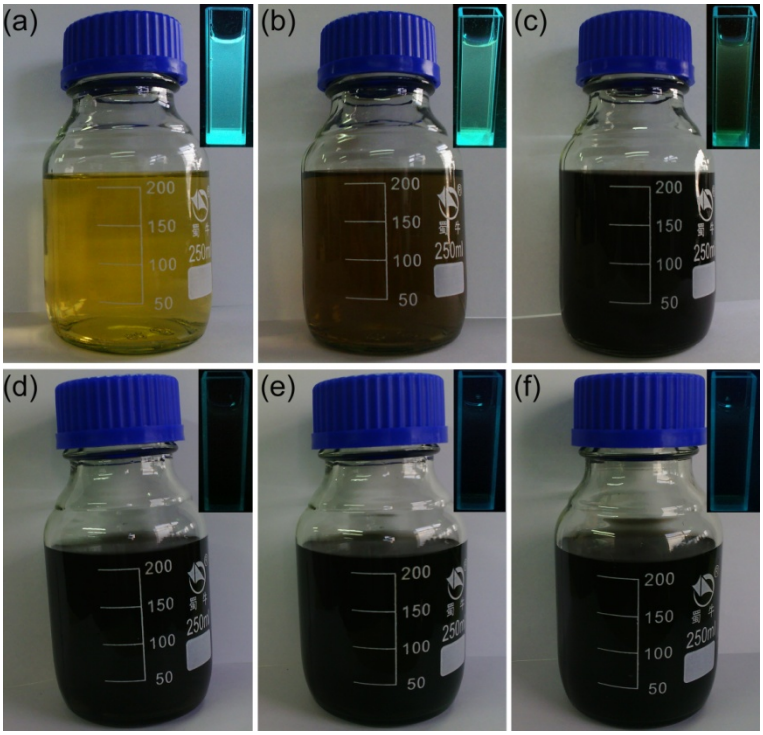

Fig. S6 photographs of different size GQDs and PRGO debris in aqueous solution captured under white light: (a) GQDs-1, (b) GQDs-2, (c) GQDs-3, (d) PRGO-1, (e) PRGO-2, and (f) PRGO-3. Insets show the corresponding photographs at 365 nm UV light.

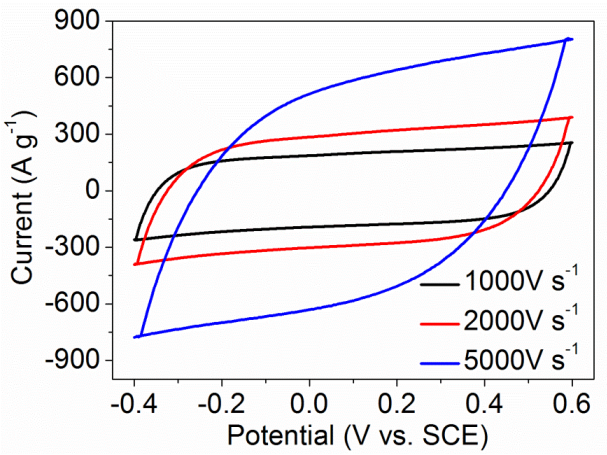

Fig. S7 CV curves of GQDs-1 at different scan rates ranging from 1000 V s^{-1} to 5000 V s^{-1}.

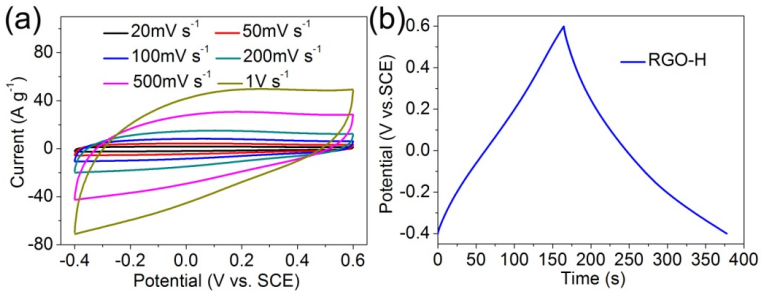

Fig. S8 (a) CV curves of RGO-H at different scan rates ranging from 20 mV s^{-1} to 1 V s^{-1}. (b) GCD curve of RGO-H at a current density of 0. 5 A g^{-1}.

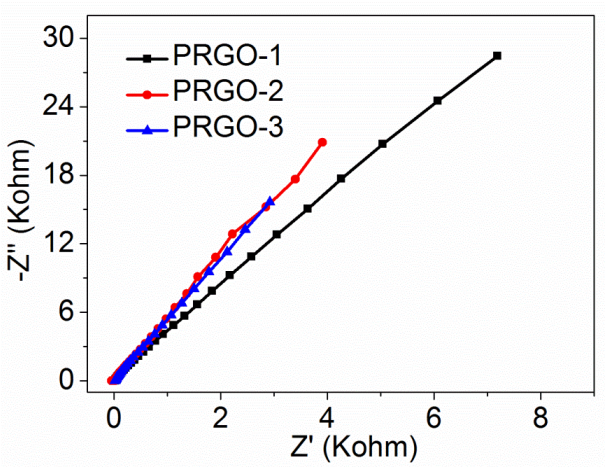

Fig. S9 Nyquist plots of PRGO debris with different sizes.

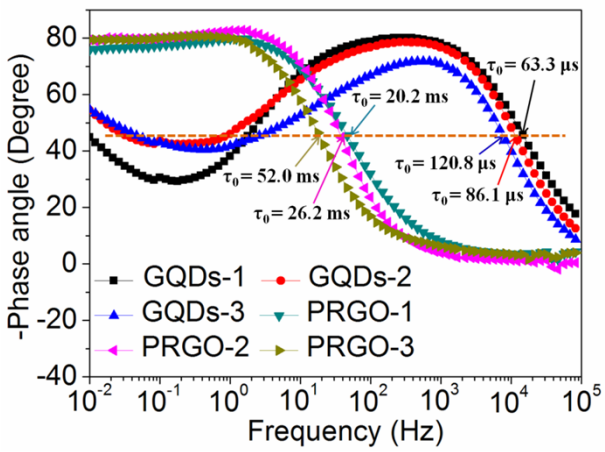

Fig. S10 Plot of impedance phase angle versus frequency.

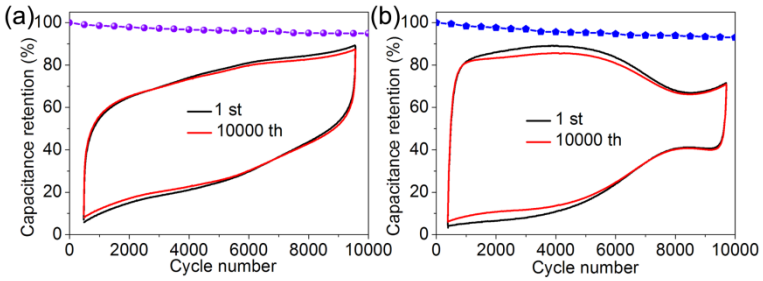

Fig. S11 Cycling stability of GQDs-1 and PRGO-3 at a scan rate of 10 V s^{-1} for 10000 cycles. Insets show the corresponding CV curves of the 1st and 10000th (10 V s^{-1} for GQDs-1, 1 V s^{-1} for PRGO-3).